The Viscosity and Thermal Conductivity Coefficients of Gaseous and Liquid Argon

B. A. Younglove and H. J. M. Hanley

Thermophysics Division, National Engineering Laboratory, National Bureau of Standards, Boulder, Colorado 80303

Received April 1, 1986; revised manuscript received August 3, 1986

Data for the viscosity and thermal conductivity of gaseous and liquid argon have been evaluated and represented by empirical functions. Tables for the viscosity from 86 to 500 K for pressures to 400 MPa, and for the thermal conductivity from 90 to 500 K for pressures to 200 MPa are presented. For the viscosity, uncertainties of 2% or better for pressures below 100 MPa, and 3% for higher pressures are assigned. For the thermal conductivity the uncertainties are 4% for temperatures below 150 K and 3% or better for temperatures above. The enhancement in the conductivity close to the critical point has been accounted for. The status of the argon transport data and the philosophy of fitting them are reviewed.

Key words: argon; correlation; critical point behavior; data evaluation; thermal conductivity; viscosity.

Contents

List of Tables

List of Figures

Nomenclature

T	temperature, K
p	pressure, MPa

ρ	density, mol/L
η	viscosity, μPa·s
η_0	dilute gas viscosity
$\Delta\eta$	dense gas and liquid viscosity
$\bar{\eta}$	critical region background viscosity
GV(i) ($i = 1,9$)	dilute gas viscosity equation parameters
XV(i) ($i = 1,13$)	dense gas and liquid viscosity equation parameters
λ	thermal conductivity, mW/m·K
λ_0	dilute gas thermal conductivity
$\Delta\lambda$	dense gas and liquid thermal conductivity
$\Delta x'$	excess transport property
GT(i) ($i = 1,9$)	dilute gas thermal conductivity equation parameters
XT(i) ($i = 1,13$)	dense gas and liquid thermal conductivity equation parameters
$\Delta\lambda_c$	critical region excess thermal conductivity
χ_T	compressibility
k_B	Boltzmann's constant
Ξ_0	length parameter, critical point thermal conductivity
ξ	length parameter, critical point viscosity
c	critical point variable subscript
*	reduced variable superscript
q_0,ϕ	critical point viscosity equation parameters
$E,\beta,\gamma,\delta,x_0$	critical point thermal conductivity parameters
$G(i)$ ($i = 1,32$), *GAMMA*	Benedict–Webb–Rubin equation parameters
R	gas constant

1. Introduction

We present a recorrelation of the viscosity (η) and thermal conductivity (λ) coefficients of argon. Recent advances in experimentation, with substantial progress in automation and data reduction techniques, are a motivation for a reassessment of transport data. In the 1974 correlation reported in this Journal,[1] for example, we pointed out that the status of thermal conductivity data was poor but that a new technique—the transient hot wire—had been introduced and showed promise. The transient hot wire method is now standard[2,3] and a relatively new technique for viscosity—the vibrating wire[4,5]—has attracted attention and could well become one of the most convenient methods to measure that coefficient.

A strong justification for an up-to-date evaluation of argon comes from theory—from computer simulation, to be precise. The technique of molecular dynamics, which has long been an essential adjunct to the study of fluids in equilibrium, can now be used to simulate the behavior of a liquid under shear or in the presence of a temperature gradient and can lead to theoretical estimates of the viscosity and thermal conductivity, respectively. Details are given in Refs. 6–8. The most extensive computer results simulate argon.[9] Although reworking the properties of argon goes against today's trend to emphasize the properties of more complex fluids, the computer simulations reveal that nonequilibrium behavior of even a fluid of spherical particles is far from simple. Such a fluid can display many of the non-Newtonian characteristics usually associated only with fluids of complex structure.[6]

Other reasons which make a recorrelation of argon desirable include: (a) a modification of the equation of state used in Ref. 1; (b) the recent publication of a reliable systematic approach to calculate the behavior of the thermal conductivity and the viscosity in the critical region; and (c) publication of consistent dilute gas coefficients.

This work will show that a really satisfactory correlation of the transport properties of argon, the simplest fluid, is still elusive. For instance there are gaps in experimental coverage, notably for the conductivity at temperatures below about twice the critical temperature; the independent estimates of the dilute gas values are not necessarily consistent with corresponding moderately dense gas and liquid data; the region in temperature and density of the anomaly in the thermal conductivity around the critical point is not resolved.[10]

One should refer to Ref. 1 for a list of the literature published before 1973 and the philosophy and criteria we use for data selection and evaluation. We have made the following judgements: (1) only those literature sources published through December 1982 are considered with the exception that we include some recent important thermal conductivity data reported in Ref. 25; (2) the correlation incorporates the equation of state of Stewart, Jacobsen, and Becker[11]; (3) the fits are constrained to the dilute gas values of Kestin *et al.*[12]; (4) thermal conductivity data close to the critical point are not correlated; rather they are calculated according to the procedure of Sengers, Basu, and Levelt Sengers[13]; (5) the anomaly in the viscosity will be discussed but the effects will not include it in the correlation: the anomaly is only seen very close to the critical point and the uncertainty in the viscosity data overrides the effect; (6) we will attempt a global correlation—i.e., a correlation over a wide range of temperature and density—realizing that some sets of data may not be fitted to within their assigned accuracy. The necessity to include inferior data at the extremes of the experimental range may well cause small systematic deviations elsewhere.

2. Data

2.1. Sources

The literature was searched for experimental argon transport data reported between January 1973 and December 1982, excluding those publications that give only data on the dilute gas. The results were: for viscosity, Refs. 14–16;

for thermal conductivity, Refs. 17–23, an earlier paper (not listed in Ref. 1), Ref. 24, and a recent paper, Ref. 25.

We were hoping that the data coverage of the earlier work could be extended. It turns out that Refs. 14 and 15 give results from the relatively new vibrating wire technique and Ref. 15 extends the density range. Reference 16 also gives an isotherm over a wide density range. References 17–20 discuss thermal conductivity results from the reliable transient hot wire method, not included in Ref. 1, but the temperature is limited to near 300 K. Reference 25 extends the temperature to 429 K from that procedure, however.

The data considered here are, therefore, Refs. 14–25 and the data selected previously,[1] namely Refs. 26–31 for the viscosity and Refs. 32–34 for the conductivity.

2.2. Data Evaluation

As in all our transport correlation papers, the data are evaluated in four stages. The first stage involves routine manipulation of the data.

We need an equation of state because the data are assessed and correlated in terms of the variable temperature (T) and density (ρ), but they are most often presented in terms of temperature and pressure (p). Accordingly, the experimental data were reformated as a function of T and ρ using the Benedict–Webb–Rubin (BWR) equation of Ref. 11, reproduced in the Appendix. If appropriate, we then compared the estimated densities for a given data set with those reported by the authors. This step led us to reject the high-density, low-temperature 223 K isotherm of Ref. 15, since density deviations of 10% or greater were noted. (We are not necessarily claiming that our densities are correct, rather that the 223 K data are inconsistent with the BWR equation.)

The next step was to construct excess function tables and curves. The excess transport property $\Delta x'$, where $x \equiv \eta$ or λ, is defined as $\Delta x'(\rho,T) = x(\rho,T) - x_0(T)$, where $x_0(T)$ is the dilute gas value. This function is used because it is close to being independent of the temperature and one can use plots of $\Delta x'$ versus ρ to check on the internal consistency of a given data set and to judge how a given set compares with those from other sources. Actually, our experience with many fluids is that there is a small but definite temperature dependence with $(\partial \Delta\eta'/\partial T)_\rho$ negative and $(\partial \Delta\lambda'/\partial T)_\rho$ positive.

We calculated dilute gas values in the range $50 \leqslant T\,\mathrm{K} \leqslant 3273$ from the formulas in Appendix C of Ref. 12 and then fitted them to the function forms used in Ref. 1 and our other work:

$$\eta_0 = \mathrm{GV}(1)T^{-1} + \mathrm{GV}(2)T^{-2/3} + \mathrm{GV}(3)T^{-1/3} + \mathrm{GV}(4) + \mathrm{GV}(5)T^{1/3} + \mathrm{GV}(6)T^{2/3} + \mathrm{GV}(7)T + \mathrm{GV}(8)T^{4/3} + \mathrm{GV}(9)T^{5/3}, \quad (1)$$

$$\lambda_0 = \mathrm{GT}(1)T^{-1} + \mathrm{GT}(2)T^{-2/3} + \mathrm{GT}(3)T^{-1/3} + \mathrm{GT}(4) + \mathrm{GT}(5)T^{1/3} + \mathrm{GT}(6)T^{2/3} + \mathrm{GT}(7)T + \mathrm{GT}(8)T^{4/3} + \mathrm{GT}(9)T^{5/3}. \quad (2)$$

The coefficients for Eqs. (1) and (2), GV(i) and GT(i), are given in Table I. The average absolute deviation for the fits above 80 K for both coefficients was 0.01%; the maximum percent deviation was 0.04% for the viscosity and 0.07% for the thermal conductivity, well within the 0.1% estimated uncertainty of the value of Ref. 12. Therefore, having $\eta_0(T)$ and $\lambda_0(T)$, we constructed excess function curves for the data. On the basis of these curves, the data of Ref. 21 which appeared 5% low, and of Ref. 23 which appeared uniformly high were eliminated from further consideration. In any case, most of the results of Ref. 23 would not be considered because, like those of Ref. 22, we do not consider data close to the critical point.

The next stage is an objective study of the papers (or papers referenced therein) based on the criteria listed in Ref. 1. This stage is almost always unsatisfactory in that the necessary experimental details are not often reported. Based on the material presented, we find the estimate of $\pm$ 2% accuracy claimed by Ref. 14 to be unsubstantiated. Reference 15 also claims $\pm$ 2%, but 3%–4% is a more consistent figure based on excess function comparisons with other authors. The thermal conductivity papers are quite detailed. We exclude Ref. 20 since the results are superceded by those of Ref. 19. The authors of Ref. 17 claim a $\pm$ 1% accuracy, whereas those of Ref. 19 claim $\pm$ 0.3%; both of these sets of results are for the isotherm at 300.65 K. On the basis of the content

TABLE. 1. Coefficients for Eqs. (1) and (2) for the dilute gas viscosity and thermal conductivity, respectively. Units: η, μPa·s; λ, mW/(m·K).

GV(1)	=	-0.8973188257E+05
GV(2)	=	0.8259113473E+05
GV(3)	=	-0.2756475915E+05
GV(4)	=	0.3068539784E+04
GV(5)	=	0.4553103615E+03
GV(6)	=	-0.1793443839E+03
GV(7)	=	0.2272225106E+02
GV(8)	=	-0.1350672796E+01
GV(9)	=	0.3183693230E-01
GT(1)	=	-0.6700976192E+05
GT(2)	=	0.6152255283E+05
GT(3)	=	-0.2049218286E+05
GT(4)	=	0.2216966254E+04
GT(5)	=	0.3579189325E+03
GT(6)	=	-0.1364658914E+03
GT(7)	=	0.1718671649E+02
GT(8)	=	-0.1018933154E+01
GT(9)	=	0.2397996932E-01

of the papers, we cannot dispute these figures, but the two sets differ by about 1.2% at intermediate densities. Reference 18 is also fairly detailed and we estimate the results to be accurate to 1%. The authors of Ref. 25 argue their data are accurate to 0.3% and we agree with their estimate. [As an aside, the two thermal conductivity papers[18,19] give weight to the result that the dilute gas Eucken factor ($\sim\eta_0/\lambda_0$) is within 0.2% of unity—the kinetic theory value—which tends to support the fact that the thermal conductivity data are accurate to that figure. But, as noted by Nieto de Castro and Roder,[17] this assessment is not necessarily upheld for all densities.]

The final step is subjective. Our assessment of the data is based on our experience working with transport data of the various authors, for argon and for other fluids; our knowledge of the apparatuses involved; and especially, the opinions of the experimentalists. Also the need for the correlation is an important factor in data selection. Since we have already published Ref. 1 in 1974, we consider a prime purpose of this work is to extend the range covered there. For this reason we will include the results of Amirkhanov *et al.*[35] at low temperatures and high densities, even though we excluded this reference from Ref. 1. [We also use the data of Ref. 14 to help establish the saturated liquid viscosity curve at high densities.] Table 2 summarizes the data selected for this correlation.

3. Correlation

We write:

$$\eta(\rho,T) = \eta_0(T) + \Delta\eta(\rho,T), \tag{3}$$

$$\lambda(\rho,T) = \lambda_0(T) + \Delta\lambda(\rho,T) + \Delta\lambda_c(\rho,T), \tag{4}$$

where $\Delta\eta$ and $\Delta\lambda$ are terms that account principally for the density dependence of the coefficients, and $\Delta\lambda_c(\rho,T)$ is the term for the thermal conductivity critical enhancement. [Equations (3) and (4) differ from those used in our earlier work in that we do not separate directly the contributions of the first density correction.]

The objective is to fit $\Delta\eta$ and $\Delta\lambda$ for the data sets of Table 2 (with data around the critical region excluded) to within the estimated accuracy of the data sets. We first tried the exponential functions used in Ref. 1 and in all our work published in this Journal. The functions gave quite satisfactory fits overall, but we were unable to eliminate some systematic error patterns at high densities. Extensions of the functions led to only modest improvements. We therefore decided to consider alternatives, and eventually selected the following:

$$\Delta\eta = \sum_{i=1}^{4} f_i\rho^i/(1+f_5\rho), \tag{5}$$

$$\Delta\lambda = \sum_{i=1}^{4} t_i\rho^i(1+t_5\rho), \tag{6}$$

where

$$\begin{aligned} f_1 &= \mathrm{XV}(1) + \mathrm{XV}(2)/T, \\ f_2 &= \mathrm{XV}(3) + \mathrm{XV}(4)/T + \mathrm{XV}(5)/T^2, \\ f_3 &= \mathrm{XV}(6) + \mathrm{XV}(7)/T + \mathrm{XV}(8)/T^2, \\ f_4 &= \mathrm{XV}(9) + \mathrm{XV}(10)/T + \mathrm{XV}(11)/T^2, \\ f_5 &= \mathrm{XV}(12) + \mathrm{XV}(13)/T. \end{aligned} \tag{7}$$

Table 2. Selected references

Authors	Approximate Experimental Range	Estimated Accuracy	Apparatus*
	VISCOSITY		
Trappeniers, et al.[15]	300-323 K:		
	100-897 MPa.	± 3%	VW
Vermesse and	308 K:		
Vidal[16]	12-606 MPa.	± 2%	CF
Kestin, Paykoc and	298 K:		
Sengers[26]	pressures to 10 MPa.	± 0.4%	OD
Haynes[27]	85-298 K:		
	pressures to 34 MPa.	± 2%	TOC
Kestin and	295-537 K:		
Whitelaw[28]	pressures to 14 MPa.	± 1%	OD
Michels, et al.[29]	273-348 K:		
	pressures to 200 MPa.	± 2%	CF
Gracki, et al.[30]	173-298 K:		
	pressures to 17 MPa.	± 1%	CF
Boon, et al.[31]	84-89 K:		
	saturated liquid.	± 3%	CF
[Abachi, et al.[14]	saturated liquid,	± 5%	VW]
	temperature below 90 K		
	only.		
	THERMAL CONDUCTIVITY		
Nieto de Castro and	301 K:		
Roder[17]	pressures to 68 MPa.	1%	THW
Clifford, et al.[18]	314-371 K:		
	pressures to 17 MPa.	1%	THW
Kestin, et al.[19]	300 K:		
	pressures to 35 MPa.	0.3%	THW
Haran, et al.[25]	300-430 K:		
	pressures to 10 MPa.	0.3%	THW
Michels, Sengers and	273-348 K:		
van de Klundert[32]	pressures to 200 MPa.	1.5%	PP
Le Neindre[33]	298-977 K:		
	pressures to 126 MPa.	4%	CC
Ziebland and	93-195 K:		
Burton[34]	pressures to 12 MPa.	4%	CC
[Amirkhanov, et al.[35]	113-223 K:		
	densities greater than	5%	CC]
	~ 30 m/ℓ only.		

* VW = vibrating wire; CF = capillary flow; OD = oscillating disc; TOC = torsional oscillating crystal; THW = transient hot wire; PP = parallel plate; CC = concentric cylinder.

Similarly, for t_i:

$$\begin{aligned} t_1 &= \mathrm{XT}(1) + \mathrm{XT}(2)/T, \\ t_2 &= \mathrm{XT}(3) + \mathrm{XT}(4)/T + \mathrm{XT}(5)/T^2, \\ t_3 &= \mathrm{XT}(6) + \mathrm{XT}(7)/T + \mathrm{XT}(8)/T^2, \\ t_4 &= \mathrm{XT}(9) + \mathrm{XT}(10)/T + \mathrm{XT}(11)/T^2, \\ t_5 &= \mathrm{XT}(12) + \mathrm{XT}(13)/T. \end{aligned} \tag{8}$$

The data were weighted following the standard expression, i.e., the weight of the jth point W_j is $1/\sigma_j$. The mean square deviation σ_j is

$$\sum_i^n \left(\frac{\partial y}{\partial x_i}\sigma_x\right)^2 + \sigma_y^2.$$

Here, y is η or λ and σ_y is the accuracy given in Table 2. We considered the errors σ_x to be caused only by errors in density and temperature and experience has shown that the latter can be neglected: σ_ρ can be set as 1 part in 2000. The derivatives $(\partial\eta/\partial\rho)_T$ and $(\partial\lambda/\partial\rho)_\lambda$ are more difficult to assess but increase very strongly with density. It must be understood, however, that we have to use empirical expressions for $\eta(\rho,T)$ and $\lambda(\rho,T)$. This, together with the fact that the distribution of points is uneven, means that W_j can be adjusted. The important criterion is that the fit should be able to reproduce the data to within their estimated accuracies, or that one must come up with a plausible reason why it does not (see Sec. 3.2). The coefficients of Eqs. (5)–(8) are given in Table 3.

Table 3. Coefficients for Eqs. (5)-(8)

Viscosity [μPa·s], thermal conductivity [mW/(m·K)], density [mol/L], and temperature [K]

XV(1) =	0.5927733783E+00	XV(2) =	-0.4251221169E+02
XV(3) =	-0.2698477165E-01	XV(4) =	0.3727762288E+02
XV(5) =	-0.3958508720E+04	XV(6) =	0.3636730841E-02
XV(7) =	-0.2633471347E+01	XV(8) =	0.2936563322E+03
XV(9) =	-0.3811869019E-04	XV(10) =	0.4451947464E-01
XV(11) =	-0.5385874487E+01	XV(12) =	-0.1115054926E-01
XV(13) =	-0.1328893444E+01		
XT(1) =	0.1536300190E+01	XT(2) =	-0.2332533199E+03
XT(3) =	-0.3027085824E-01	XT(4) =	0.1896279196E+02
XT(5) =	0.1054230664E+02	XT(6) =	0.2588139028E-04
XT(7) =	-0.4546798772E+00	XT(8) =	0.4320206998E+01
XT(9) =	0.1593643304E-04	XT(10) =	0.1262253904E-03
XT(11) =	-0.2937213042E-02	XT(12) =	-0.2262773007E-01
XT(13) =	-0.1445619495E+00		

3.1. The Critical Point

All our previous correlations in this Journal have discussed the estimation of the term $\Delta\lambda_c(\rho,T)$ of Eq. (4). There is no need to repeat those remarks here. As noted in the Introduction, we follow exactly the procedure outlined by Sengers, Basu, and Levelt Sengers in Table IX of Ref. 13. Define:

$$\begin{aligned}
T^* &= T/T_c,\\
\rho^* &= \rho/\rho_c,\\
p^* &= p/p_c,\\
\Delta T^* &= (T-T_c)/T_c,\\
\Delta\rho^* &= (\rho-\rho_c)/\rho_c,\\
\chi_T^* &= \rho\left(\frac{\partial\rho}{\partial p}\right)_T\left(\frac{p_c}{\rho_c^2}\right),\\
x &= \Delta T^*/|\Delta\rho^*|^{1/\beta},\\
y &= (x+x_0)/x_0,
\end{aligned} \tag{9}$$

where the subscript c denotes the critical value and β and x_0 are coefficients. Then, Eq. (4.2) of Ref. 13 becomes for argon,

$$\Delta\lambda_c = \frac{1.02k_B p_c}{\Xi_0 6\pi\eta}\left(\frac{T^*}{\rho^*}\right)^2\left(\frac{\partial p^*}{\partial T^*}\right)^2_{\rho^*}(\chi_T^*)^{0.46807} \times\exp\{-[39.8(\Delta T^*)^2+5.45(\Delta\rho^*)^4]\}, \tag{10}$$

where Ξ_0 is a length parameter and k_B is Boltzmann's constant. The viscosity is calculated from Eqs. (1) and (5) and the derivatives $(\partial p/\partial T)_\rho$ and $(\partial p/\partial\rho)_T$ from the BWR equation of state unless $|\Delta\rho^*|\leqslant 0.25$ and $|\Delta T^*|\leqslant 0.03$. If both of these conditions are satisfied, χ_T^* is evaluated from the scaled equation of state,

$$\chi_t^* = (0.0813)(\Delta t^*)^{-\gamma},$$

for $\Delta\rho^* = 0$, or

$$\chi_T^* = |\Delta\rho^*|^{-\gamma/\beta} \times\frac{[(1+E)/(1+Ey^{2\beta})]^{(\gamma-1)/2\beta}}{D[\delta+(y-1)(\delta-\beta^{-1}+Ey^{2\beta})/(1+Ey^{2\beta})]}, \tag{11}$$

where D, E, γ, and δ are coefficients. We defer to Refs. 13 and 36 for discussions on these critical point equations. The parameters required are given in Table 4. Figure 1 shows the effect at three temperatures.

Table 4. Parameters used in the critical point Eqs. (9)-(11)

p_c	=	4.9058 MPa
ρ_c	=	13.410 mol/L
T_c	=	150.86 K
Ξ_0	=	$6.0795 * 10^{10}$ m
γ	=	1.190
β	=	0.355
D	=	2.43
E	=	0.287
x_0	=	0.183
δ	=	4.352

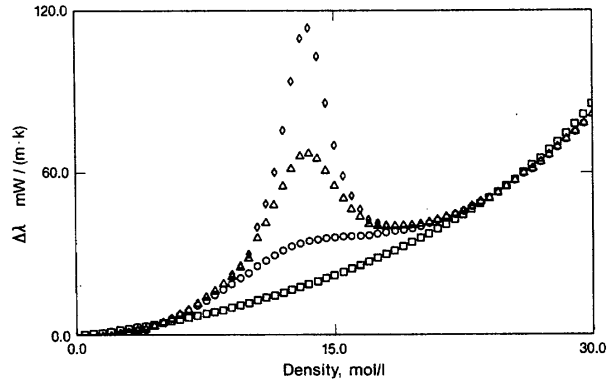

FIG. 1. The excess thermal conductivity of argon at three temperatures close to critical compared to the background ($T_c = 150.860$ K): (□) background, (○) 155.0 K, (△) 151.5 K, (◇) 151.06 K.

The anomalous behavior of the viscosity around the critical point will not be included in this correlation: the enhancement is negligible unless one is within ~0.02% of the critical temperature. As a matter of interest, however, some calculations are reported. Basu and Sengers[13,37] propose a simple equation

$$\eta = \bar{\eta}(0.53 q_0 \xi)^{\phi}, \tag{12}$$

where $\bar{\eta}$ is the viscosity at the temperature and density of interest without the enhancement, ξ is a correlation length—which equals $(\chi_T^*)^{0.532}\, 6.08\times 10^{-10}$ m for argon—which is a measure of the range of density fluctuations in the fluid, q_0 is an adjustable fluid dependent constant, and ϕ is, in principle, a fluid independent exponent. Given the appropriate viscosity data, a plot of $\ln \eta/\bar{\eta}$ versus ξ will yield q_0 and ϕ (if ϕ is also to be treated as adjustable). Suitable data are unavailable for argon, so we cannot evaluate q_0 and ϕ directly but Basu and Sengers estimate $q_0 = 0.032\times 10^{-10}$ m^{-1} with $\phi = 0.065$ for nitrogen from nitrogen data. Argon values can be approximated by scaling q_0 via the ratios of the critical densities to give

$$\eta = \bar{\eta}[0.02(10^{-10})\xi\,]^{0.065}. \tag{12a}$$

Viscosity plots for three temperatures within 0.02% of the critical are shown in Fig. 2.

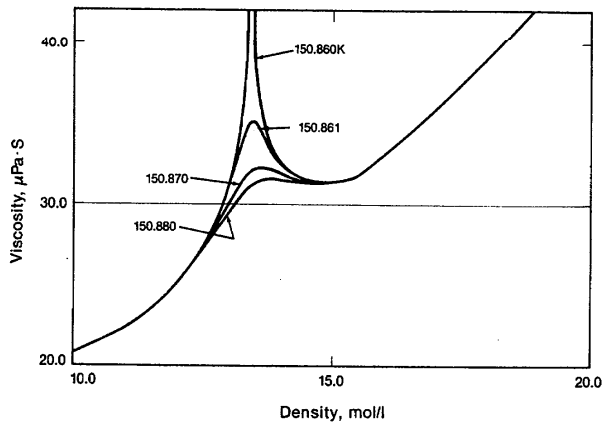

FIG. 2. The viscosity of argon from Eq. (12a) very close to the critical temperature.

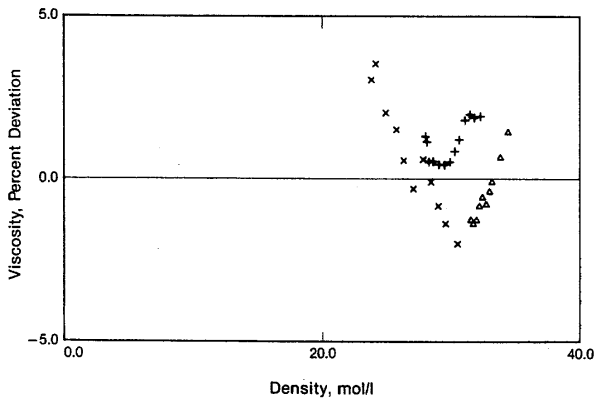

FIG. 3. Viscosity deviations at low temperatures from Ref. 27: (△) 107.7 K, (+) 125 K, (×) 139.7 K.

3.2. Deviation Curves

Deviation curves for the viscosity and thermal conductivity are presented in Figs. 3–10 and 11–16, respectively. Percent deviation is defined as (expt − calc)100/expt, where the calculated values are from Eqs. (1), (5), and (7) for the viscosity and Eqs. (2), (6), (8), and (10) for the conductivity. The average absolute deviations of the fits were 0.99% for 506 points, and 1.84% for 884 points, respectively. We have been successful in fitting the majority of the data to within their estimated accuracy and this is a satisfactory result considering the range in temperature and density covered. Isotherms have been grouped to observe better possible systematic deviations with temperature and density. The curves are fairly self-explanatory, but we have the following comments.

(1) Comparisons between the viscosity and thermal conductivity data sets emphasize that the latter is the less complete. Thermal conductivity isotherms at low temperatures are missing, as are data for the thermal conductivity saturated liquid boundary, although Ref. 34 reports data that are close. It would also be more desirable not to have sole author coverage at the limits of the temperature range for both coefficients; e.g., the viscosity results for $T < 173$ K are from Ref. 16 and the thermal conductivity for high temperatures are from Ref. 33.

(2) There is a systematic pattern in the viscosity deviation curves at densities greater than about 25 mol/L. It is

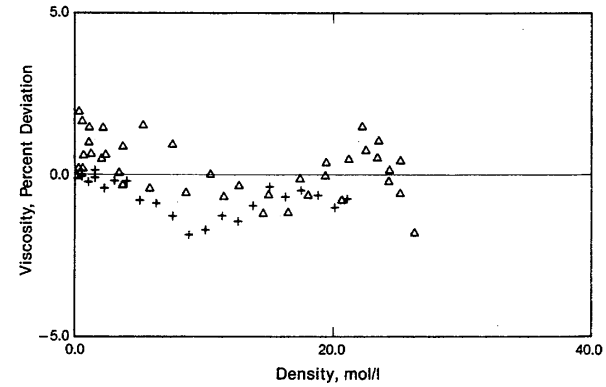

FIG. 4. Viscosity deviations at 173 K from Ref. 27 (△) and Ref. 30 (+).

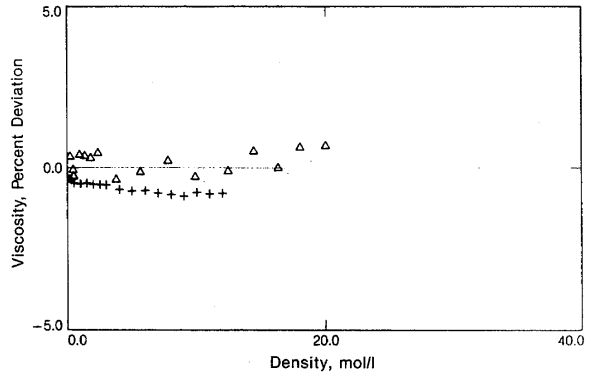

FIG. 5. Viscosity deviations at 223 K from Ref. 27 (△) and Ref. 30 (+).

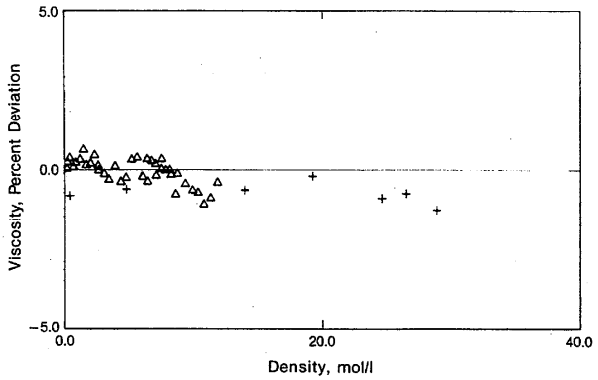

FIG. 6. Viscosity deviations at 270 K from Ref. 27 (△) and Ref. 29 (+).

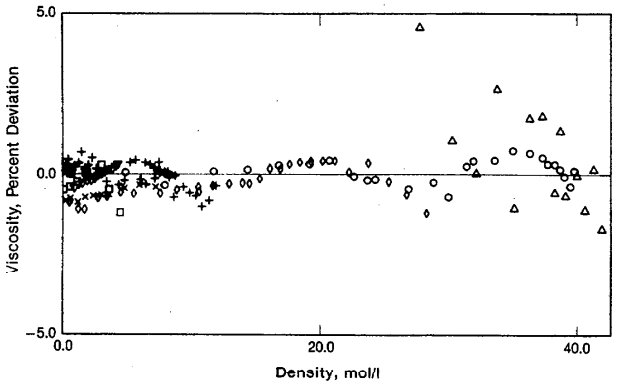

FIG. 7. Viscosity deviations at 300 K from Ref. 15 (△), Ref. 16 (○), Ref. 27 (+), Ref. 30 (×), Ref. 29 (◇), Ref. 26 (▽), and Ref. 28 (□).

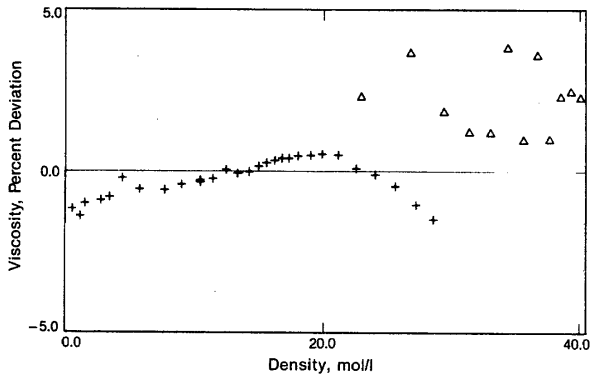

FIG. 8. Viscosity deviations at 323 K from Ref. 15 (△) and Ref. 29 (+).

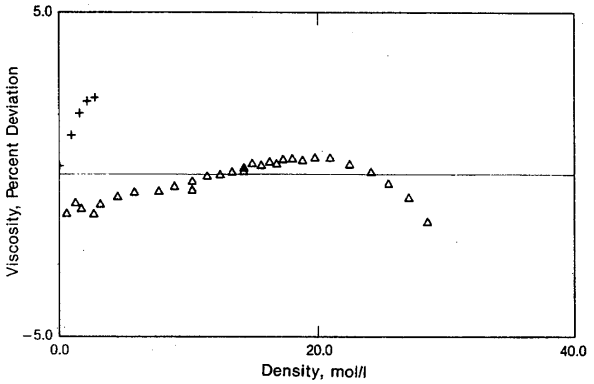

FIG. 9. Viscosity deviations at high temperatures from Ref. 29 at 348 K (△) and Ref. 28 at 537 K (+).

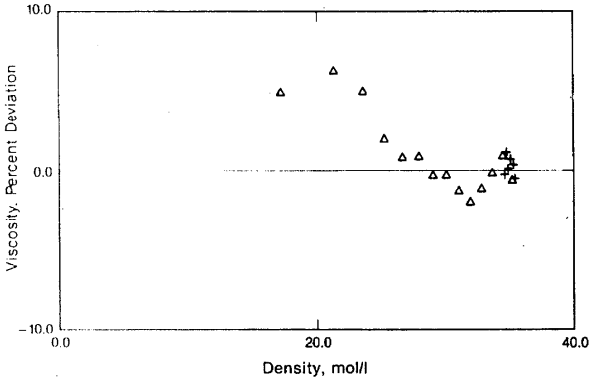

FIG. 10. Viscosity deviations for the saturated liquid from Ref. 27 (△) and Ref. 31 (+).

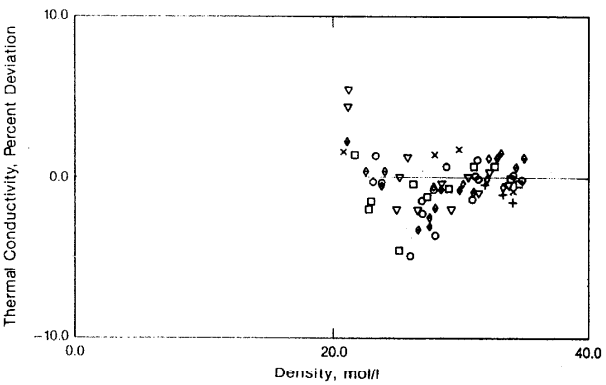

FIG. 11. Thermal conductivity deviations at various pressures close to saturations from the data of Ref. 34. Approximate pressures in MPa: (▽) 4.7, (⊖) 12, (×) 1.8, (□) 7, (○) 9.5, (+) 1, (◇) 2.4.

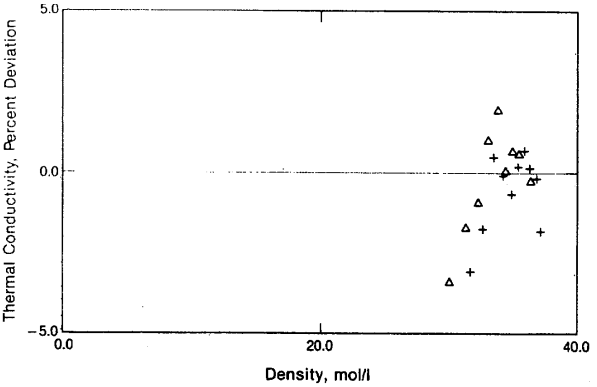

FIG. 12. Thermal conductivity deviations at low temperatures from Ref. 35; (+) 113 K, (△) 122 K.

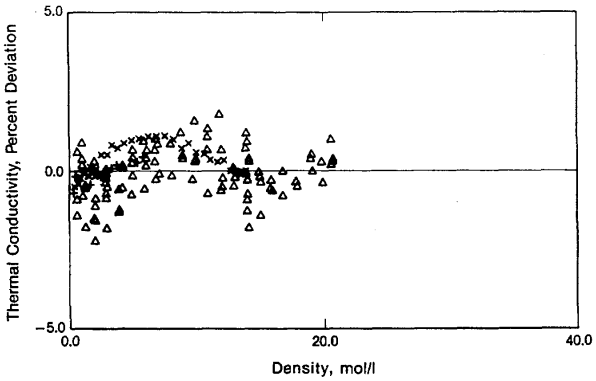

FIG. 13a. Thermal conductivity at $T \sim 300$ K from various authors; Ref. 17 (△), Ref. 18 (+), Ref. 19 (×).

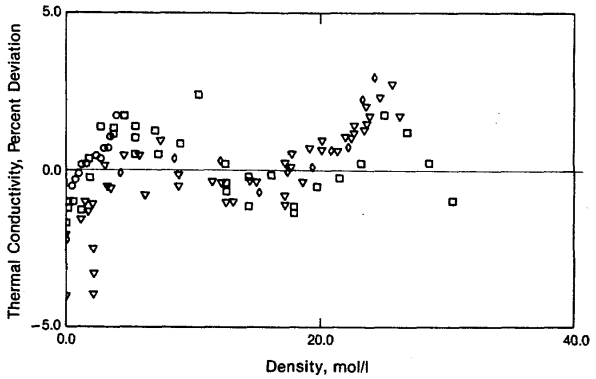

FIG. 13b. Thermal conductivity at $T \sim 300$ K (continued); Ref. 25 (○), Ref. 32 (□), Ref. 33a (◇), Ref. 33b (▽).

not clear why this is so. The several empirical functions we have tried cannot smooth it out and fit satisfactorily data for the lower densities. We should point out that data for fluids other than argon from the torsionally oscillating crystal at low temperatures and high densities show the behavior represented by Fig. 3, so systematic experimental error may contribute. Constraining the viscosity fit to the dilute gas values of Ref. 12 will introduce a small systematic error but not enough to account for the patterns. A very possible explanation is that our functional forms do not have the correct temperature dependence. We have verified that the derivative $(\partial \Delta\eta/\partial T)_\rho$ is negative but that may simply be a necessary condition. Nevertheless, we do not feel the accuracy in the data justify using a more complex function.

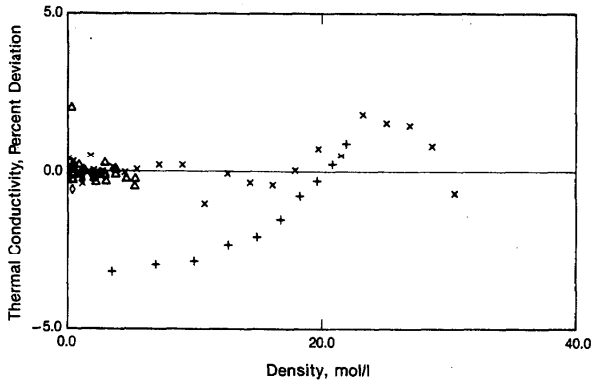

FIG. 14. Thermal conductivity at temperatures between 347 and 352 K from Ref. 18 (△) 348–352 K, Ref. 25 (◇) 337 K, Ref. 32 (×) 348 K, Ref. 33a (+) 348 K.

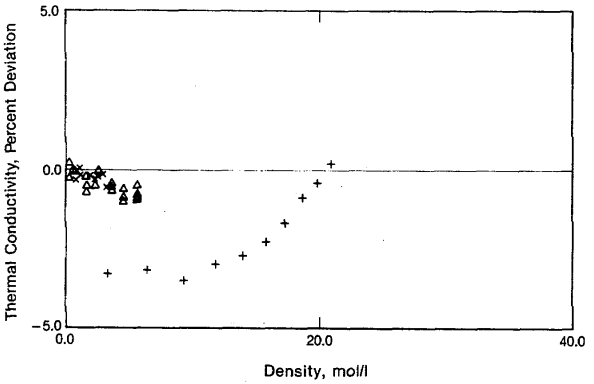

FIG. 15. Thermal conductivity at $T \sim 370$ K from Ref. 18 (△), Ref. 25 (×) and Ref. 33a (+).

(3) The conductivity deviation patterns are not entirely satisfactory since the data of Refs. 17–19 and 25 are known to be precise and accurate: there is a small but definite systematic deviation between experiment and the correlation. We can speculate as to why. As for the viscosity, the global correlating function may not be good enough, in fact, it would be surprising if it were. The deviation may be caused in part by the influence of data representing other regions of the ρ–T phase diagram. These data are less accurate than that of Refs. 17–19 and 25 but we have argued that they have to be considered. Constraining the fit to the dilute gas values of Ref. 12 will cause some systematic error. There is also the possible influence of the critical point anomaly to consider. Roder contends that this influence extends to about twice the critical temperature for oxygen,[10] methane,[38] and ethane[39] and Nieto de Castro and Roder argue that it influences the interpretation of argon data at 300 K. If the argument is correct, our functional form would not be complete and would underestimate the conductivity by approximately 1% between $0.3\,\rho_c$ and $1.13\,\rho_c$.

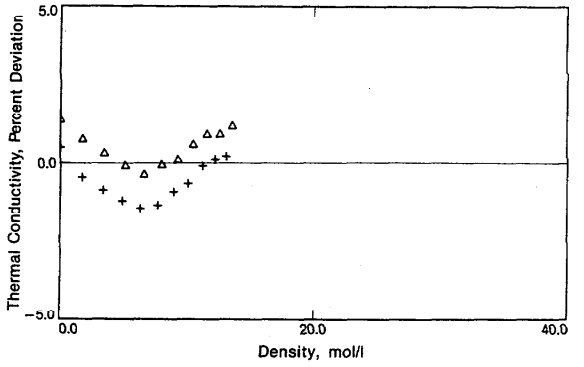

FIG. 16. Thermal conductivity at high temperatures from Ref. 33a: (△) 646 K, (+) 674 K.

TABLE 5. Viscosity of argon in μPa·s

	P, MPa									
T, K	.1	.5	1.0	1.5	2.0	2.5	3.0	3.5	4.0	5.0
86.0	270.0	271.0	272.1	273.3	274.4	275.6				
90.0	7.2	240.0	241.0	242.1	243.2	244.3	245.4	246.4	247.5	249.6
95.0	7.6	209.6	210.7	211.7	212.8	213.9	214.9	216.0	217.0	219.1
100.0	8.0	184.1	185.2	186.3	187.4	188.4	189.5	190.5	191.6	193.7
105.0	8.4	162.1	163.2	164.3	165.4	166.5	167.5	168.6	169.6	171.7
110.0	8.8	8.9	143.8	145.0	146.1	147.2	148.3	149.3	150.4	152.5
115.0	9.1	9.3	126.5	127.7	128.9	130.0	131.2	132.3	133.4	135.5
120.0	9.5	9.7	9.8	112.1	113.4	114.6	115.8	116.9	118.1	120.3
125.0	9.9	10.1	10.2	10.5	99.1	100.4	101.7	103.0	104.2	106.6
130.0	10.4	10.5	10.6	10.9	11.2	87.1	88.6	90.0	91.4	94.0
135.0	10.8	10.9	11.0	11.3	11.6	12.1	75.8	77.5	79.1	82.1
140.0	11.2	11.3	11.4	11.7	12.0	12.4	13.0	64.7	66.9	70.7
145.0	11.6	11.7	11.9	12.1	12.3	12.7	13.2	14.0	52.8	58.8
150.0	12.0	12.1	12.3	12.5	12.7	13.1	13.5	14.1	15.0	42.9
155.0	12.4	12.5	12.7	12.9	13.1	13.4	13.8	14.3	15.0	17.7
160.0	12.8	12.9	13.1	13.3	13.5	13.8	14.1	14.6	15.1	16.9
165.0	13.2	13.3	13.5	13.6	13.9	14.1	14.5	14.9	15.3	16.7
170.0	13.6	13.7	13.8	14.0	14.2	14.5	14.8	15.2	15.6	16.7
175.0	14.0	14.1	14.2	14.4	14.6	14.9	15.2	15.5	15.9	16.8
180.0	14.4	14.5	14.6	14.8	15.0	15.2	15.5	15.8	16.2	17.0
185.0	14.8	14.9	15.0	15.2	15.4	15.6	15.8	16.1	16.5	17.3
190.0	15.1	15.2	15.4	15.6	15.7	16.0	16.2	16.5	16.8	17.5
195.0	15.5	15.6	15.8	15.9	16.1	16.3	16.5	16.8	17.1	17.8
200.0	15.9	16.0	16.1	16.3	16.5	16.7	16.9	17.1	17.4	18.0
205.0	16.3	16.4	16.5	16.7	16.8	17.0	17.2	17.5	17.7	18.3
210.0	16.7	16.8	16.9	17.0	17.2	17.4	17.6	17.8	18.1	18.6
215.0	17.0	17.1	17.3	17.4	17.6	17.7	17.9	18.1	18.4	18.9
220.0	17.4	17.5	17.6	17.8	17.9	18.1	18.3	18.5	18.7	19.2
225.0	17.8	17.9	18.0	18.1	18.3	18.4	18.6	18.8	19.0	19.5
230.0	18.1	18.2	18.3	18.5	18.6	18.8	19.0	19.1	19.3	19.8
235.0	18.5	18.6	18.7	18.8	19.0	19.1	19.3	19.5	19.7	20.1
240.0	18.8	18.9	19.0	19.2	19.3	19.5	19.6	19.8	20.0	20.4
245.0	19.2	19.3	19.4	19.5	19.7	19.8	20.0	20.1	20.3	20.7
250.0	19.5	19.6	19.7	19.9	20.0	20.1	20.3	20.5	20.6	21.0
255.0	19.9	20.0	20.1	20.2	20.3	20.5	20.6	20.8	20.9	21.3
260.0	20.2	20.3	20.4	20.5	20.7	20.8	20.9	21.1	21.3	21.6
265.0	20.6	20.6	20.7	20.9	21.0	21.1	21.3	21.4	21.6	21.9
270.0	20.9	21.0	21.1	21.2	21.3	21.4	21.6	21.7	21.9	22.2
275.0	21.2	21.3	21.4	21.5	21.6	21.8	21.9	22.1	22.2	22.5
280.0	21.6	21.6	21.7	21.9	22.0	22.1	22.2	22.4	22.5	22.8
285.0	21.9	22.0	22.1	22.2	22.3	22.4	22.5	22.7	22.8	23.1
290.0	22.2	22.3	22.4	22.5	22.6	22.7	22.9	23.0	23.1	23.4
295.0	22.5	22.6	22.7	22.8	22.9	23.0	23.2	23.3	23.4	23.7
300.0	22.9	22.9	23.0	23.1	23.2	23.4	23.5	23.6	23.7	24.0
310.0	23.5	23.6	23.7	23.8	23.9	24.0	24.1	24.2	24.3	24.6
320.0	24.1	24.2	24.3	24.4	24.5	24.6	24.7	24.8	24.9	25.2
330.0	24.7	24.8	24.9	25.0	25.1	25.2	25.3	25.4	25.5	25.8
340.0	25.3	25.4	25.5	25.6	25.7	25.8	25.9	26.0	26.1	26.3
350.0	25.9	26.0	26.1	26.2	26.3	26.4	26.5	26.6	26.7	26.9
360.0	26.5	26.6	26.7	26.8	26.9	27.0	27.0	27.1	27.2	27.5
370.0	27.1	27.2	27.3	27.4	27.4	27.5	27.6	27.7	27.8	28.0
380.0	27.7	27.8	27.8	27.9	28.0	28.1	28.2	28.3	28.4	28.6
390.0	28.3	28.3	28.4	28.5	28.6	28.7	28.7	28.8	28.9	29.1
400.0	28.8	28.9	29.0	29.1	29.1	29.2	29.3	29.4	29.5	29.7
410.0	29.4	29.5	29.5	29.6	29.7	29.8	29.9	29.9	30.0	30.2
420.0	30.0	30.0	30.1	30.2	30.2	30.3	30.4	30.5	30.6	30.7
430.0	30.5	30.6	30.6	30.7	30.8	30.9	30.9	31.0	31.1	31.3
440.0	31.0	31.1	31.2	31.2	31.3	31.4	31.5	31.5	31.6	31.8
450.0	31.6	31.6	31.7	31.8	31.8	31.9	32.0	32.1	32.1	32.3
460.0	32.1	32.2	32.2	32.3	32.4	32.4	32.5	32.6	32.7	32.8
470.0	32.6	32.7	32.8	32.8	32.9	33.0	33.0	33.1	33.2	33.3
480.0	33.2	33.2	33.3	33.3	33.4	33.5	33.5	33.6	33.7	33.8
490.0	33.7	33.7	33.8	33.9	33.9	34.0	34.1	34.1	34.2	34.3
500.0	34.2	34.2	34.3	34.4	34.4	34.5	34.6	34.6	34.7	34.8

TABLE 5. Viscosity of argon in μPa·s—Continued

	P, MPa									
T, K	6.0	7.0	8.0	9.0	10.0	15.0	20.0	30.0	40.0	50.0
90.0	251.8	253.9	256.0	258.1	260.3					
95.0	221.2	223.3	225.3	227.4	229.4	239.5	249.5			
100.0	195.7	197.8	199.8	201.8	203.8	213.6	223.2	242.1		
105.0	173.8	175.8	177.8	179.8	181.8	191.5	200.8	218.9	236.6	
110.0	154.6	156.6	158.7	160.7	162.6	172.2	181.3	198.8	215.6	232.2
115.0	137.6	139.7	141.8	143.8	145.8	155.3	164.3	181.3	197.4	213.2
120.0	122.5	124.7	126.8	128.8	130.8	140.3	149.2	165.8	181.5	196.6
125.0	108.9	111.1	113.3	115.4	117.4	127.0	135.9	152.2	167.4	181.9
130.0	96.5	98.8	101.1	103.3	105.4	115.2	124.0	140.1	154.9	168.9
135.0	84.9	87.5	89.9	92.3	94.5	104.6	113.5	129.3	143.7	157.3
140.0	73.9	76.9	79.6	82.1	84.5	95.0	104.0	119.7	133.8	146.9
145.0	63.1	66.7	69.8	72.6	75.2	86.3	95.4	111.0	124.8	137.6
150.0	51.4	56.4	60.3	63.6	66.6	78.3	87.7	103.3	116.8	129.3
155.0	34.6	45.3	50.8	54.9	58.4	71.1	80.7	96.3	109.6	121.8
160.0	21.1	31.9	40.7	46.3	50.5	64.5	74.3	89.9	103.0	114.9
165.0	19.1	23.8	31.2	38.0	43.0	58.4	68.6	84.2	97.1	108.8
170.0	18.4	21.2	25.6	31.1	36.4	53.0	63.4	79.0	91.8	103.2
175.0	18.2	20.2	23.1	27.0	31.3	48.1	58.7	74.3	86.9	98.0
180.0	18.2	19.8	21.9	24.7	28.0	43.8	54.5	70.1	82.4	93.4
185.0	18.3	19.6	21.3	23.4	26.0	40.2	50.8	66.2	78.4	89.1
190.0	18.4	19.5	21.0	22.7	24.7	37.1	47.6	62.7	74.7	85.2
195.0	18.6	19.6	20.8	22.3	24.0	34.7	44.7	59.6	71.4	81.7
200.0	18.8	19.7	20.8	22.0	23.5	32.9	42.2	56.8	68.3	78.4

	P, MPa									
T, K	6.0	7.0	10.0	20.0	30.0	50.0	75.0	100.0	200.0	400.0
200.0	18.8	19.7	23.5	42.2	56.8	78.4	100.5			
205.0	19.0	19.8	23.2	40.1	54.3	75.4	97.0	116.6		
210.0	19.3	20.0	23.0	38.4	52.0	72.7	93.8	112.8		
215.0	19.5	20.2	22.9	36.9	50.0	70.1	90.8	109.4		
220.0	19.8	20.4	22.9	35.6	48.2	67.8	88.0	106.2		
225.0	20.0	20.6	23.0	34.6	46.6	65.7	85.4	103.2		
230.0	20.3	20.9	23.0	33.7	45.1	63.7	83.0	100.4		
235.0	20.6	21.1	23.1	33.0	43.9	62.0	80.8	97.7		
240.0	20.9	21.4	23.3	32.5	42.8	60.3	78.7	95.3		
245.0	21.2	21.6	23.4	32.0	41.8	58.8	76.7	93.0		
250.0	21.4	21.9	23.6	31.6	40.9	57.4	74.9	90.8		
255.0	21.7	22.2	23.8	31.3	40.1	56.1	73.2	88.8		
260.0	22.0	22.4	24.0	31.1	39.4	54.9	71.7	86.9		
265.0	22.3	22.7	24.2	30.9	38.9	53.8	70.2	85.1		
270.0	22.6	23.0	24.4	30.7	38.3	52.8	68.8	83.4		
275.0	22.9	23.3	24.6	30.6	37.9	51.9	67.5	81.8		
280.0	23.2	23.5	24.8	30.5	37.5	51.1	66.3	80.4		
285.0	23.5	23.8	25.0	30.5	37.1	50.3	65.2	78.9		
290.0	23.7	24.1	25.3	30.5	36.8	49.6	64.1	77.6		
295.0	24.0	24.4	25.5	30.5	36.6	48.9	63.2	76.4		
300.0	24.3	24.6	25.7	30.5	36.4	48.3	62.2	75.2		
310.0	24.9	25.2	26.2	30.6	36.0	47.3	60.6	73.0	119.4	
320.0	25.5	25.7	26.7	30.8	35.8	46.4	59.1	71.1	115.9	
330.0	26.0	26.3	27.2	31.0	35.7	45.7	57.8	69.3	112.7	
340.0	26.6	26.8	27.7	31.3	35.6	45.1	56.6	67.7	109.7	
350.0	27.1	27.4	28.2	31.6	35.7	44.6	55.6	66.3	107.0	187.1
360.0	27.7	27.9	28.7	31.9	35.7	44.1	54.8	65.1	104.5	182.3
370.0	28.2	28.5	29.2	32.2	35.8	43.8	54.0	64.0	102.2	177.8
380.0	28.8	29.0	29.7	32.6	36.0	43.6	53.3	62.9	100.1	173.6
390.0	29.3	29.5	30.2	32.9	36.2	43.4	52.7	62.0	98.1	169.6
400.0	29.9	30.1	30.7	33.3	36.4	43.2	52.2	61.2	96.3	165.9
410.0	30.4	30.6	31.2	33.7	36.6	43.2	51.8	60.5	94.6	162.5
420.0	30.9	31.1	31.7	34.1	36.8	43.1	51.4	59.8	93.0	159.3
430.0	31.4	31.6	32.2	34.5	37.1	43.1	51.1	59.3	91.5	156.2
440.0	32.0	32.1	32.7	34.9	37.4	43.2	50.9	58.7	90.2	153.4
450.0	32.5	32.6	33.2	35.3	37.7	43.2	50.7	58.3	88.9	150.7
460.0	33.0	33.1	33.7	35.7	38.0	43.3	50.5	57.9	87.7	148.1
470.0	33.5	33.6	34.2	36.1	38.3	43.4	50.3	57.5	86.6	145.7
480.0	34.0	34.1	34.6	36.5	38.7	43.6	50.3	57.2	85.6	143.4
490.0	34.5	34.6	35.1	36.9	39.0	43.7	50.2	56.9	84.6	141.3
500.0	35.0	35.1	35.6	37.3	39.3	43.9	50.1	56.7	83.7	139.2

TABLE 6. Thermal conductivity of argon in mW/(m·K)

	P, MPa									
T, K	.1	.5	1.0	1.5	2.0	2.5	3.0	3.5	4.0	5.0
90.0	5.5	124.3	124.6	124.9	125.1	125.4	125.6	125.9	126.2	126.7
95.0	5.8	116.9	117.2	117.5	117.8	118.1	118.4	118.7	118.9	119.5
100.0	6.1	109.9	110.3	110.6	111.0	111.3	111.6	111.9	112.3	112.9
105.0	6.4	103.3	103.6	104.0	104.4	104.8	105.2	105.5	105.9	106.6
110.0	6.8	6.5	97.1	97.6	98.0	98.4	98.9	99.3	99.7	100.5
115.0	7.1	6.9	90.6	91.1	91.6	92.1	92.6	93.1	93.6	94.5
120.0	7.4	7.2	7.1	84.6	85.2	85.8	86.3	86.9	87.4	88.5
125.0	7.7	7.6	7.5	7.5	78.6	79.2	79.9	80.5	81.2	82.4
130.0	8.0	8.0	7.9	8.0	8.2	72.3	73.2	74.0	74.7	76.2
135.0	8.4	8.3	8.3	8.4	8.6	9.3	65.9	66.9	67.9	69.7
140.0	8.7	8.7	8.7	8.8	9.0	9.5	10.8	59.3	60.6	62.9
145.0	9.0	9.0	9.0	9.2	9.4	9.8	10.7	12.7	53.2	56.0
150.0	9.3	9.3	9.4	9.5	9.7	10.1	10.8	12.0	14.7	50.4
155.0	9.6	9.7	9.7	9.9	10.1	10.4	10.9	11.8	13.4	21.7
160.0	10.0	10.0	10.1	10.2	10.4	10.7	11.2	11.8	12.8	17.0
165.0	10.3	10.3	10.4	10.6	10.8	11.0	11.4	11.9	12.7	15.2
170.0	10.6	10.7	10.8	10.9	11.1	11.3	11.6	12.1	12.6	14.4
175.0	10.9	11.0	11.1	11.2	11.4	11.6	11.9	12.3	12.7	14.1
180.0	11.2	11.3	11.4	11.6	11.7	11.9	12.2	12.5	12.9	14.0
185.0	11.5	11.6	11.7	11.9	12.1	12.3	12.5	12.8	13.1	14.0
190.0	11.8	11.9	12.0	12.2	12.4	12.6	12.8	13.1	13.4	14.2
195.0	12.1	12.2	12.4	12.5	12.7	12.9	13.1	13.4	13.7	14.4
200.0	12.4	12.5	12.7	12.8	13.0	13.2	13.4	13.7	14.0	14.6
205.0	12.7	12.8	13.0	13.1	13.3	13.5	13.7	14.0	14.2	14.9
210.0	13.0	13.1	13.3	13.4	13.6	13.8	14.0	14.3	14.5	15.1
215.0	13.3	13.4	13.6	13.7	13.9	14.1	14.3	14.5	14.8	15.4
220.0	13.6	13.7	13.8	14.0	14.2	14.4	14.6	14.8	15.1	15.6
225.0	13.9	14.0	14.1	14.3	14.5	14.7	14.9	15.1	15.4	15.9
230.0	14.2	14.3	14.4	14.6	14.8	15.0	15.2	15.4	15.6	16.1
235.0	14.4	14.6	14.7	14.9	15.1	15.2	15.4	15.7	15.9	16.4
240.0	14.7	14.8	15.0	15.2	15.3	15.5	15.7	15.9	16.2	16.7
245.0	15.0	15.1	15.3	15.4	15.6	15.8	16.0	16.2	16.4	16.9
250.0	15.3	15.4	15.5	15.7	15.9	16.1	16.3	16.5	16.7	17.2
255.0	15.5	15.7	15.8	16.0	16.2	16.3	16.5	16.7	17.0	17.4
260.0	15.8	15.9	16.1	16.2	16.4	16.6	16.8	17.0	17.2	17.7
265.0	16.1	16.2	16.3	16.5	16.7	16.9	17.1	17.3	17.5	17.9
270.0	16.3	16.5	16.6	16.8	17.0	17.1	17.3	17.5	17.7	18.2
275.0	16.6	16.7	16.9	17.0	17.2	17.4	17.6	17.8	18.0	18.4
280.0	16.8	17.0	17.1	17.3	17.5	17.7	17.8	18.0	18.2	18.7
285.0	17.1	17.2	17.4	17.6	17.7	17.9	18.1	18.3	18.5	18.9
290.0	17.4	17.5	17.6	17.8	18.0	18.2	18.3	18.5	18.7	19.1
295.0	17.6	17.7	17.9	18.1	18.2	18.4	18.6	18.8	19.0	19.4
300.0	17.9	18.0	18.2	18.3	18.5	18.7	18.8	19.0	19.2	19.6
310.0	18.4	18.5	18.6	18.8	19.0	19.2	19.3	19.5	19.7	20.1
320.0	18.9	19.0	19.1	19.3	19.5	19.6	19.8	20.0	20.2	20.5
330.0	19.3	19.5	19.6	19.8	19.9	20.1	20.3	20.5	20.6	21.0
340.0	19.8	19.9	20.1	20.3	20.4	20.6	20.7	20.9	21.1	21.5
350.0	20.3	20.4	20.6	20.7	20.9	21.0	21.2	21.4	21.5	21.9
360.0	20.8	20.9	21.0	21.2	21.3	21.5	21.7	21.8	22.0	22.3
370.0	21.2	21.3	21.5	21.6	21.8	22.0	22.1	22.3	22.4	22.8
380.0	21.7	21.8	21.9	22.1	22.2	22.4	22.6	22.7	22.9	23.2
390.0	22.1	22.2	22.4	22.5	22.7	22.8	23.0	23.1	23.3	23.6
400.0	22.6	22.7	22.8	23.0	23.1	23.3	23.4	23.6	23.7	24.1
410.0	23.0	23.1	23.3	23.4	23.6	23.7	23.9	24.0	24.2	24.5
420.0	23.4	23.5	23.7	23.8	24.0	24.1	24.3	24.4	24.6	24.9
430.0	23.9	24.0	24.1	24.3	24.4	24.5	24.7	24.8	25.0	25.3
440.0	24.3	24.4	24.5	24.7	24.8	25.0	25.1	25.3	25.4	25.7
450.0	24.7	24.8	25.0	25.1	25.2	25.4	25.5	25.7	25.8	26.1
460.0	25.1	25.2	25.4	25.5	25.6	25.8	25.9	26.1	26.2	26.5
470.0	25.5	25.6	25.8	25.9	26.1	26.2	26.3	26.5	26.6	26.9
480.0	25.9	26.1	26.2	26.3	26.5	26.6	26.7	26.9	27.0	27.3
490.0	26.4	26.5	26.6	26.7	26.9	27.0	27.1	27.3	27.4	27.7
500.0	26.8	26.9	27.0	27.1	27.2	27.4	27.5	27.6	27.8	28.0

TABLE 6. Thermal conductivity of argon in mW/(m·K)—Continued

	P, MPa									
T, K	6.0	7.0	8.0	9.0	10.0	15.0	20.0	30.0	40.0	50.0
90.0	127.2	127.7	128.2	128.7	129.2					
95.0	120.1	120.7	121.2	121.7	122.3	124.8	127.2			
100.0	113.5	114.2	114.8	115.4	116.0	118.8	121.4	126.3		
105.0	107.3	108.0	108.7	109.3	110.0	113.1	116.0	121.4	126.3	
110.0	101.3	102.0	102.8	103.5	104.2	107.7	110.8	116.6	121.9	126.8
115.0	95.3	96.2	97.0	97.8	98.6	102.4	105.8	112.0	117.6	122.8
120.0	89.4	90.4	91.3	92.2	93.1	97.2	100.9	107.4	113.3	118.8
125.0	83.5	84.6	85.7	86.7	87.7	92.1	96.1	103.0	109.2	114.9
130.0	77.5	78.8	80.0	81.1	82.2	87.2	91.4	98.8	105.2	111.1
135.0	71.4	72.9	74.3	75.6	76.8	82.3	86.9	94.6	101.3	107.4
140.0	64.9	66.8	68.4	70.0	71.4	77.5	82.4	90.6	97.5	103.8
145.0	58.5	60.6	62.5	64.3	65.9	72.7	78.1	86.7	93.9	100.3
150.0	52.6	54.9	57.0	58.9	60.7	68.1	73.9	82.9	90.4	96.9
155.0	46.3	49.7	52.1	54.1	56.0	63.7	69.8	79.3	87.0	93.7
160.0	27.3	40.3	46.2	49.3	51.5	59.5	65.9	75.8	83.7	90.5
165.0	20.4	28.5	36.7	42.4	46.1	55.7	62.2	72.5	80.6	87.5
170.0	17.5	22.3	28.3	34.2	39.2	51.7	58.7	69.3	77.6	84.6
175.0	16.1	19.2	23.2	27.8	32.5	47.6	55.3	66.3	74.8	81.9
180.0	15.5	17.6	20.4	23.8	27.6	43.2	52.0	63.4	72.0	79.3
185.0	15.2	16.8	18.9	21.5	24.4	39.2	48.7	60.7	69.4	76.7
190.0	15.2	16.5	18.1	20.2	22.5	35.7	45.6	58.1	67.0	74.4
195.0	15.3	16.4	17.8	19.4	21.3	33.0	42.8	55.6	64.7	72.1
200.0	15.4	16.4	17.6	19.0	20.6	30.8	40.3	53.3	62.5	69.9

	P, MPa								
T, K	6.0	7.0	10.0	20.0	30.0	50.0	75.0	100.0	200.0
200.0	15.4	16.4	20.6	40.3					
205.0	15.6	16.5	20.2	38.2					
210.0	15.8	16.7	20.0	36.4	49.2				
215.0	16.0	16.8	19.8	34.8	47.5				
220.0	16.3	17.0	19.8	33.5	45.8				
225.0	16.5	17.2	19.8	32.5	44.4				
230.0	16.7	17.4	19.8	31.5	43.0				
235.0	17.0	17.6	19.9	30.8	41.8				
240.0	17.2	17.8	20.0	30.1	40.7				
245.0	17.4	18.0	20.1	29.6	39.8				
250.0	17.7	18.2	20.2	29.2	38.9				
255.0	17.9	18.5	20.3	28.8	38.1				
260.0	18.2	18.7	20.5	28.5	37.5	52.1			
265.0	18.4	18.9	20.7	28.3	36.8	51.2			
270.0	18.6	19.1	20.8	28.1	36.3	50.3			
275.0	18.9	19.4	21.0	28.0	35.8	49.5			
280.0	19.1	19.6	21.2	27.9	35.4	48.8			
285.0	19.3	19.8	21.3	27.8	35.1	48.1			
290.0	19.6	20.0	21.5	27.7	34.7	47.5			
295.0	19.8	20.2	21.7	27.7	34.4	46.9			
300.0	20.0	20.5	21.9	27.7	34.2	46.3	58.8		
310.0	20.5	20.9	22.3	27.7	33.8	45.3	57.4		
320.0	20.9	21.3	22.7	27.8	33.5	44.5	56.2	66.4	
330.0	21.4	21.8	23.0	27.9	33.3	43.8	55.1	65.0	
340.0	21.8	22.2	23.4	28.1	33.2	43.2	54.1	63.7	
350.0	22.3	22.6	23.8	28.3	33.1	42.7	53.3	62.6	
360.0	22.7	23.1	24.2	28.5	33.1	42.3	52.5	61.6	
370.0	23.1	23.5	24.6	28.7	33.1	41.9	51.8	60.7	92.6
380.0	23.5	23.9	25.0	28.9	33.2	41.6	51.2	59.9	91.0
390.0	24.0	24.3	25.3	29.2	33.3	41.4	50.7	59.1	89.4
400.0	24.4	24.7	25.7	29.4	33.4	41.2	50.2	58.4	88.0
410.0	24.8	25.1	26.1	29.7	33.5	41.1	49.8	57.8	86.7
420.0	25.2	25.5	26.5	30.0	33.6	41.0	49.5	57.2	85.4
430.0	25.6	25.9	26.9	30.2	33.8	40.9	49.2	56.7	84.3
440.0	26.0	26.3	27.2	30.5	34.0	40.9	48.9	56.3	83.2
450.0	26.4	26.7	27.6	30.8	34.2	40.8	48.7	55.9	82.1
460.0	26.8	27.1	28.0	31.1	34.4	40.9	48.5	55.5	81.2
470.0	27.2	27.5	28.3	31.4	34.6	40.9	48.3	55.2	80.3
480.0	27.6	27.8	28.7	31.7	34.8	40.9	48.2	54.9	79.5
490.0	27.9	28.2	29.1	32.0	35.0	41.0	48.1	54.7	78.7
500.0	28.3	28.6	29.4	32.3	35.2	41.1	48.0	54.4	78.0

Table 7. Argon properties at saturation

Temp K	Pressure MPa	Density mol/l	Thermal Conductivity mW/(m·K)	Viscosity μPa·s
90.0	.134	34.455	124.0	238.7
92.0	.163	34.139	120.9	225.9
94.0	.196	33.818	118.0	214.1
96.0	.233	33.492	115.2	203.2
98.0	.277	33.160	112.4	193.0
100.0	.325	32.822	109.7	183.4
102.0	.380	32.478	107.0	174.4
104.0	.441	32.127	104.4	165.8
106.0	.509	31.769	101.8	157.7
108.0	.585	31.404	99.3	150.0
110.0	.668	31.031	96.7	142.8
112.0	.759	30.650	94.2	135.8
114.0	.859	30.259	91.7	129.2
116.0	.968	29.859	89.1	122.9
118.0	1.087	29.447	86.6	116.9
120.0	1.216	29.024	84.1	111.1
122.0	1.355	28.587	81.6	105.6
124.0	1.505	28.135	79.1	100.3
126.0	1.667	27.665	76.6	95.2
128.0	1.841	27.176	74.0	90.2
130.0	2.027	26.664	71.4	85.4
132.0	2.227	26.125	68.8	80.8
134.0	2.441	25.554	66.1	76.2
136.0	2.668	24.944	63.4	71.8
138.0	2.911	24.286	60.8	67.4
140.0	3.170	23.566	58.2	62.9
142.0	3.446	22.765	55.8	58.5
144.0	3.740	21.851	53.6	53.9
146.0	4.053	20.767	52.0	49.1
148.0	4.386	19.383	51.2	43.6
150.0	4.743	17.205	55.3	36.5

4. Tables of Values

Having the correlating equations, the viscosity coefficients of argon have been calculated from 86 to 500 K, for pressures to 400 MPa. The thermal conductivity coefficients have been calculated from 90 to 500 K, for pressures to 200 MPa. The results are presented as Tables 5 and 6. For convenience, saturation values are given separately in Table 7. We ensured that an entry in the tables would not represent an extrapolation much beyond the range of the experimental data. An upper limit of 35.2 mol/L was selected. Above 200 K, this limit was lowered to 30.0 mol/L for the viscosity and 20.8 mol/L for the thermal conductivity. Note the pressure range reported for the conductivity is less than that for the viscosity.

We are confident that we have not introduced any significant systematic error by representing the data with the chosen correlating functions. An accuracy assessment of the tabular values can therefore be based on the accuracy of the input data. Figures 17 and 18 schematically represent the error estimates assigned. If

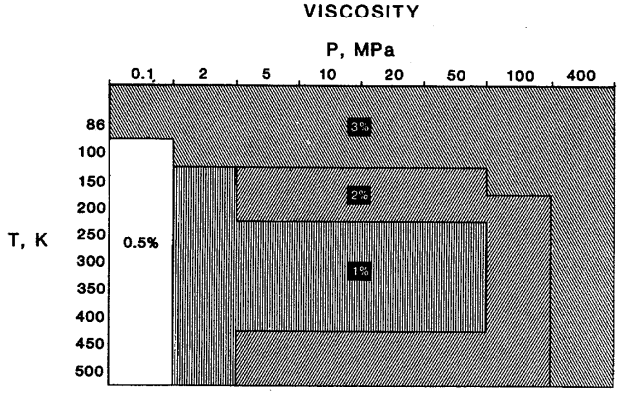

FIG. 17. Error estimates of the values of Table 5.

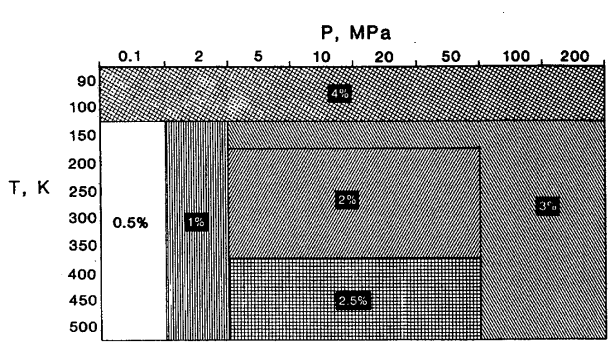

FIG. 18. Error estimates of the values of Table 6.

$$(|T - T_c|)/T_c < 0.03$$

and

$$(|\rho - \rho_c|)/\rho_c \lesssim 0.3,$$

the estimate on the thermal conductivity should be increased to $\pm$ 15%. We have also not accounted for the enhancement in the viscosity at the critical point, but one would have to be within $(|T - T_c|)/T_c$ of 10^{-3} for this effect to be significant.

5. Conclusion

We have recorrelated the viscosity and thermal conductivity coefficients of argon following the philosophy and guidelines of our previous 1974 work reported as Ref. 1. The justification is primarily that new data are available. On the other hand, this work has revealed how difficult it is to fit accurate transport data and get a satisfactory density and temperature dependence. It is almost as if one has pushed a purely empirical fit to its limits: we need more input from theory, especially on the behavior of the fluid at high densities.

The correlation has revealed that the status of the transport properties of even the simplest fluid, argon, is not entirely satisfactory. Gaps in data coverage exist, particularly for the thermal conductivity below room temperature. It would also seem advantageous to extend the range of the conductivity data reported by the transient hot wire method.

6. Acknowledgments

This work was supported by the Office of Standard Reference Data and was carried out under the auspices of the IUPAC Subcommittee on Transport Properties. We are grateful to many people for their advice: H. M. Roder, J. V. Sengers, W. A. Wakeham, J. Kestin, and C. Nieto de Castro, in particular. Karen Bowie typed the manuscript and we thank her for her help.

7. References

[1] H. J. M. Hanley, R. D. McCarty, and W. M. Haynes, J. Phys. Chem. Ref. Data 3, 979 (1974).
[2] H. M. Roder, J. Res. Natl. Bur. Stand. (U.S.) 86, 457 (1981).
[3] A. A. Clifford, J. Kestin, and W. A. Wakeham, Physica A 100, 370 (1980).

[4]E. Charles, J. Molenat, H. Abachi, J. Michel, and P. Malbrunot, J. Phys. E **13**, 829 (1980).
[5]L. Bruschi, G. Mazzi, M. Santini, and G. Torzo, J. Low Temp. Phys. **18**, 487 (1975).
[6]Phys. Today **37**(1) (1984). This issue has articles on fluids in nonequilibrium.
[7]Physica A **118** (1983). This issue reports on a conference on nonlinear fluid behavior held in Boulder, CO, 1982.
[8]W. G. Hoover, Ann. Rev. Phys. Chem. **34**, 103 (1983).
[9]H. J. M. Hanley, J. F. Ely, D. J. Evans, and S. Hess, Data available at the Thermophysics Division, Natl. Bur. Stand. (U.S.), Boulder, CO.
[10]H. M. Roder, J. Res. Natl. Bur. Stand. (U.S.) **87**, 279 (1982); J. H. Dymond, Physica A **79**, 65 (1975).
[11]R. B. Stewart, R. T. Jacobsen, and J. H. Becker, Center for Applied Thermo. Studies Report No. 81-3, University of Idaho, 1981; B. A. Younglove, J. Phys. Chem. Ref. Data Suppl. **11** (1982).
[12]J. Kestin, K. Knierim, E. A. Mason, B. Najafi, S. T. Ro, and M. Waldman, J. Phys. Chem. Ref. Data. **13**, 229 (1984).
[13]J. V. Sengers, R. S. Basu, and J. M. H. Levelt Sengers, NASA Contract. Rep. No. 3424, 1981.
[14]H. Abachi, J. Molenat, and P. Malbrunot, Phys. Lett. A **80**, 171 (1980).
[15]J. Trappeniers, P. S. Van der Gulik, and H. Van Den Hoof, Chem. Phys. Lett. **70**, 438 (1980).
[16]J. Vermesse and D. Vidal, C. R. Acad. Sci. Paris B **277**, 191 (1973).
[17]C. A. Nieto de Castro and H. M. Roder, J. Res. Natl. Bur. Stand. **86**, 293 (1981).
[18]A. A. Clifford, P. Gray, A. I. Johns, A. C. Scott, and J. T. R. Watson, J. Chem. Soc. Faraday Trans. 1 **77**, 2679 (1981).
[19]J. Kestin, R. Paul, A. A. Clifford, and W. A. Wakeham, Physica A **100**, 349 (1980).
[20]J. J. de Groot, J. Kestin, H. Sookiazian, and W. A. Wakeham, Physica A **92**, 117 (1978).
[21]V. P. Slyusar, V. M. Tretyakov, and N. S. Rudenko, Ukr. Fiz. Zh. **22**, 1070 (1977).
[22]N. J. Trappeniers, *Proceedings of the 8th International Symposium on Thermophysical Properties*, edited by J. V. Sengers (ASME, New York, 1982), Vol. 1, p. 232.
[23]F. M. Gumerov, D. G. Amirkhanov, and A. G. Usmanov, Teplo. Mass. Khim. Tek. **7**, 8 (1979).
6
[24]A. A. Tarzimanov and V. A. Arslanov, Tr. Kazan. Khim.-Technol. Inst. **47**, 157 (1971).
[25]E. N. Haran, G. C. Maitland, M. Mustafa, and W. A. Wakeham, Ber. Buns. Phys. Chem. **87**, 657 (1983).
[26]J. Kestin, E. Paykoc, and J. V. Sengers, Physica **54**, 1 (1971).
[27]W. M. Haynes, Physica **70**, 410 (1973).
[28]J. Kestin and J. H. Whitelaw, Physica **29**, 335 (1963).
[29]A. Michels, A. Botzen, and W. Schuurman, Physica **20**, 1141 (1954).
[30]J. A. Gracki, G. P. Flynn, and J. J. Ross, J. Chem. Phys. **51**, 3856 (1969).
[31]J. P. Boon and G. Thomaes, Physica **29**, 208 (1963); J. P. Boon, J. C. Legros, and G. Thomaes, Physica **33**, 547 (1967).
[32]A. Michels, J. V. Sengers, and L. J. M. Van de Klundert, Physica **29**, 149 (1963).
[33a]B. Le Neindre, Ph.D. thesis (University of Paris, 1969).
[33b]B. Le Neindre, R. Tufeu, and P. Bury, in *Proceedings of the 8th Conference on Thermal Conductivity*, edited by C. Y. Ho and R. E. Taylor (Plenum, New York, 1969), p. 75
[34]H. Ziebland and J. T. A. Burton, Br. J. Appl. Phys. **9**, 52 (1958).
[35]K. I. Amirkhanov, A. P. Adamov, and G. D. Gasanov, Inzh-Fiz. Zh. **22**, 835 (1972).
[36]J. V. Sengers and J. M. H. Levelt Sengers, Int. J. Thermophys. **5**, 195 (1984).
[37]R. S. Basu and J. V. Sengers, J. Heat Transfer **101**, 3 (1979); R. S. Basu, J. V. Sengers, and J. T. R. Watson, Int. J. Thermophys. **1**, 33 (1980).
[38]H. M. Roder, Int. J. Thermophys. **6**, 119 (1985).
[39]H. M. Roder and C. Nieto de Castro, High Temp. High Pressures **17**, 453 (1985); R. C. Prasad, J. E. S. Venart, and N. Mani, in *Proceedings of the 18th Conference on Thermal Conductivity*, edited by T. Ashworth and D. R. Smith (Plenum, New York, 1985), p. 81.

Appendix: Argon Equation of State

The equation of state used here is that of Stewart *et al.*[11] The Benedict–Webb–Rubin form is:

$$
\begin{aligned}
p = {} & \rho RT \\
& + \rho^2[G(1)T + G(2)T^{1/2} + G(3) + G(4)/T \\
& + G(5)/T^2)] \\
& + \rho^3[G(6)T + G(7) + G(8)/T + G(9)/T^2] \\
& + \rho^4[G(10)T + G(11) + G(12)/T] + \rho^5[G(13)] \\
& + \rho^6[G(14)/T + G(15)/T^2] + \rho^7[G(16)/T] \\
& + \rho^8[G(17)/T + G(18)/T^2] + \rho^9[G(19)/T^2] \\
& + \rho^3[G(20)/T^2 + G(21)/T^3]\exp(\gamma\rho^2) \\
& + \rho^5[G(22)/T^2 + G(23)/T^4]\exp(\gamma\rho^2) \\
& + \rho^7[G(24)/T^2 + G(25)/T^3]\exp(\gamma\rho^2) \\
& + \rho^9[G(26)/T^2 + G(27)/T^4]\exp(\gamma\rho^2) \\
& + \rho^{11}[G(28)/T^2 + G(29)/T^3]\exp(\gamma\rho^2) \\
& + \rho^{13}[G(30)/T^2 + G(31)/T^3 \\
& + G(32)/T^4]\exp(\gamma\rho^2),
\end{aligned}
$$

where p is in MPa, ρ in mol/L, and T in K. The equation is constrained to the critical parameters: $T_c = 150.86$ K, $p_c = 4.9058$ MPa, and $\rho_c = 13.418$ mol/L. (Note: ρ_c differs from the value in Table 4.)

The coefficients are:

$$
\begin{aligned}
G(1) &= -0.656\,973\,129\,40\,\text{E}-04 \\
G(2) &= 0.182\,295\,780\,10\,\text{E}-01 \\
G(3) &= -0.364\,947\,014\,10\,\text{E}+00 \\
G(4) &= 0.123\,201\,210\,70\,\text{E}+02 \\
G(5) &= -0.861\,357\,827\,40\,\text{E}+03 \\
G(6) &= 0.797\,857\,969\,10\,\text{E}-05 \\
G(7) &= -0.291\,148\,911\,00\,\text{E}-02 \\
G(8) &= 0.758\,182\,175\,80\,\text{E}+00 \\
G(9) &= 0.878\,048\,816\,90\,\text{E}+03 \\
G(10) &= 0.142\,314\,598\,90\,\text{E}-07 \\
G(11) &= 0.167\,414\,613\,10\,\text{E}-03 \\
G(12) &= -0.320\,044\,790\,90\,\text{E}-01 \\
G(13) &= 0.256\,176\,637\,20\,\text{E}-05 \\
G(14) &= -0.547\,593\,494\,10\,\text{E}-04 \\
G(15) &= -0.450\,503\,205\,80\,\text{E}-01 \\
G(16) &= 0.201\,325\,465\,30\,\text{E}-05 \\
G(17) &= -0.167\,894\,127\,30\,\text{E}-07 \\
G(18) &= 0.420\,732\,927\,10\,\text{E}-04 \\
G(19) &= -0.544\,421\,299\,60\,\text{E}-06 \\
G(20) &= -0.800\,485\,501\,10\,\text{E}+03 \\
G(21) &= -0.131\,930\,420\,10\,\text{E}+05 \\
G(22) &= -0.495\,492\,393\,00\,\text{E}+01 \\
G(23) &= 0.809\,213\,217\,70\,\text{E}+04 \\
G(24) &= -0.987\,010\,406\,10\,\text{E}-02 \\
G(25) &= 0.202\,044\,156\,20\,\text{E}+00
\end{aligned}
$$

$G(26) = -0.163\,741\,720\,50\,\mathrm{E}-04$
$G(27) = -0.703\,894\,413\,60\,\mathrm{E}-01$
$G(28) = -0.115\,432\,453\,90\,\mathrm{E}-07$
$G(29) = \ \ 0.155\,599\,011\,70\,\mathrm{E}-05$
$G(30) = -0.149\,217\,853\,60\,\mathrm{E}-10$
$G(31) = -0.100\,135\,607\,10\,\mathrm{E}-08$
$G(32) = \ \ 0.293\,396\,321\,60\,\mathrm{E}-07$
$GAMMA = -0.005\,554\,237\,2$